Chapter 12
Role of Mechanical Stress in Lung Repair and Regeneration

Connie C.W. Hsia and Priya Ravikumar

Introduction

The mammalian lung and its thoracic container, bounded by the diaphragm and the rib cage and partitioned by the mediastinum, arise from distinct embryonic origins but are mechanically linked as a single functional unit of gas transport. The scaffold is essentially a suspended elastic fiber continuum stabilized by surfactant, subjected to constant and cyclic physical stresses arising from two interdependent pumps (respiratory and cardiac) that bring air and blood into close proximity over a vast interface area. From rest to peak exercise, minute ventilation can increase tenfold while blood flow through lung capillaries, the largest microvascular network in the body that receives the entire right ventricular cardiac output, can increase fivefold in elite athletes. Respiratory mechanical stresses are hardwired for transmission via elastic fibers from central airways to distal alveolar septa and the pleura, then via cell junctions and the cytoskeleton from the cell surface to the nucleus where they transduce a host of molecular and biochemical processes culminating in structural growth and remodeling. As physical tension and compression of tissue constituents is essential for maintaining whole lung integrity (termed tensegrity) [1], growth and function of the lung are mechanically constrained by the size, shape, and compliance of its container, the thorax.

In general, branching morphogenesis is the result of mechanical forces acting at an interface between two material phases (e.g., air–tissue or tissue–fluid). Inhomogeneity in either the applied force or the encountered resistance creates pressure gradients that drive iterative bronchoalveolar and vascular bifurcations until all available intrathoracic spaces are filled [2]. The characteristic fractal or "self-similar" branching networks allow efficient inspired gas delivery by convection

C.C.W. Hsia (✉) • P. Ravikumar
Department of Internal Medicine, University of Texas Southwestern Medical Center, Dallas, TX 75390-9034, USA
e-mail: Connie.Hsia@utsouthwestern.edu

to each of some 30,000 human acini, the basic units of gas exchange, and maximize the diffusion surface area of some 480 million alveolar subdivisions [3]. This anatomical plan fundamentally dictates physiology in that ventilation, perfusion, and diffusion also exhibit fractal behavior at different scales [4]. Through the modulation of intrathoracic pressures, generated passively by the opposing elastic recoil of the chest wall and the lung and actively by respiratory muscle contractions, pathophysiological changes in the lung and the thorax directly influence each other [5]. The simple fact of mechanical thoraco-pulmonary coupling leads to complex consequences on the initiation, perpetuation, and re-initiation of lung growth, remodeling, and functional outcome. In this chapter, we briefly review the nature of thoraco-pulmonary mechanical interactions and their contribution to growth, regrowth, and physiological compensation of the postnatal lung.

Mechanical Stress Modulates Lung Development

Normal respiratory development invokes nearly all of the major homeostatic signaling pathways, leading to coordinated enlargement of the rib cage, diaphragm, and lung. In the embryonic lung bud, the positive pressure exerted by tracheal luminal fluid sustains iterative airway branching. Increasing luminal pressure by tracheal ligation accelerates branching and the increase in lung size. Reducing luminal pressure has the opposite effect. Pressure-accelerated branching morphogenesis proceeds in the absence of fibroblast growth factor-10 (FGF-10), although FGF-10 expression accentuates the response [6, 7]. Respiratory movements are essential for lung maturation in later fetal life [8, 9]. Postnatal lung distention by continuous positive airway pressure [10] or perfluorocarbon instillation [11] increases lung volume and protein and DNA contents. New alveoli form predominantly at the lung periphery [12, 13] where mechanical forces are borne by the septa in the absence of major bronchovascular support. Restricted lung expansion in congenital diaphragmatic hernia causes lung hypoplasia [14]; correcting the diaphragmatic defect allows lung expansion, "*catch-up*" growth, and vascular remodeling, eventually reversing pulmonary arterial hypertension [15] and nearly normalizing lung diffusing capacity in long-term survivors [16, 17]. Temporary tracheal occlusion to increase airway luminal pressure has been used in congenital diaphragmatic hernia to enhance antenatal lung growth as a bridge to surgical repair [18]. In severe childhood kyphoscoliosis chest wall deformity restricts both lung and thorax growth [19–22]. Conversely, inhibition of lung growth may deform the growing rib cage [23].

The balance between the inward lung recoil and the outward rib cage recoil mutually determines their dimensions at a given transpulmonary pressure. During maturation, the enlarging rib cage imposes mechanical traction on lung parenchyma (Fig. 12.1). Stretching lung cells or tissue broadly increases permeability and ion flux [24, 25], signal transduction [26, 27], gene transcription [28], and cytokine release [29, 30], culminating in cell proliferation [27, 31], apoptosis [32], protein
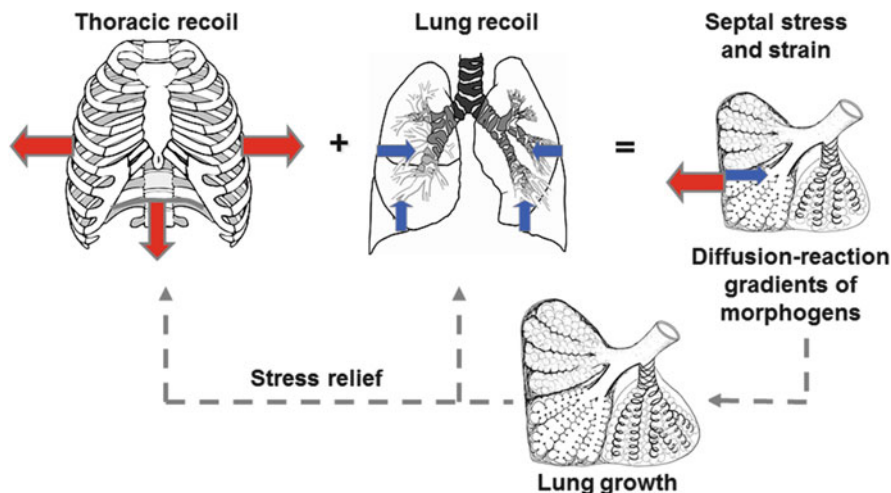
Fig. 12.1 Growth and development of the lung are mechanically coupled to that of the thorax. Adapted from [5]

turnover [24, 33, 34], and other metabolic processes. Tissue growth and remodeling in turn relieve stress and strain. Recoil of the lung exerts reciprocal traction on and modulates the growth of the rib cage. These feedback interactions continue until the closure of bony epiphyses upon reaching somatic maturity. Thereafter, mechanical signals diminish so that both the lung and the thorax stop growing [5]. Subsequent re-initiation of lung growth is possible only if the appropriate thoraco-pulmonary mechanical stress is reimposed and intrathoracic space is available for growth to occur without significant architectural distortion.

Innate Potential for Compensatory Lung Growth

Lower vertebrates such as newts and salamanders are well known for their ability to regrow a completely new and fully functional limb or tail to replace one that has been lost [35]. While mammals cannot regenerate an entire lung, under appropriate stimulation, mature mammalian lungs retain the ability to *add new gas exchange structures* including the intra-acinar airways (respiratory bronchioles, alveolar ducts, and alveolar sacs) and alveolar septa (cells, matrix, fibers, and capillaries). When some lung units are destroyed by disease or surgery, the remaining units expand under the negative intrathoracic pressure leading to unfolding of alveolar surfaces. Simultaneously, pulmonary perfusion to these units increases at a given cardiac output, leading to microvascular recruitment and augmentation of lung diffusing capacity (Fig. 12.2). As loss of lung units continues, physical stress and deformation of tissue and microvasculature exceed a critical threshold, at which point structural growth is stimulated. The newly generated cells, matrix, fibers, and
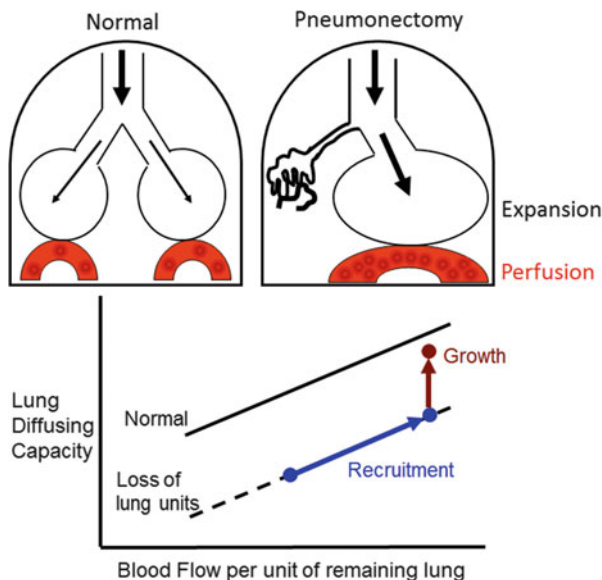
Fig. 12.2 Two types of complex mechanical signals following loss of lung units—expansion of the remaining parenchyma, and increased perfusion to the remaining microvasculature. These signals recruit alveolar-capillary volumes and surface areas, leading to a higher lung diffusing capacity as blood flow per unit of remaining lung increases (*blue line* and *symbols*). When mechanical signals exceed a threshold intensity, structural growth is stimulated with a further increase in lung diffusing capacity at any given pulmonary blood flow above that expected per unit of initially remaining lung

capillaries undergo *remodeling* or architectural adjustment of the alveolar septa, fibroelastic scaffold, and broncho-vasculature, ultimately leading to balanced increases in all major acinar components. Remodeling is a critical step that redistributes mechanical stress, maximizes air–tissue and tissue–blood interface areas, minimizes tissue–blood barrier resistance to diffusion, and optimizes ventilation-to-perfusion and perfusion-to-diffusion matching. The end result is a larger gas exchanger with a higher lung diffusing capacity above that expected from the initially remaining fraction of lung units under a given set of conditions, thus achieving the goal of *functional compensation* (Fig. 12.2). Conversely, generation of structural components that fail to directly or indirectly support the functional goal is not compensatory growth.

## Pneumonectomy Model of Compensatory Lung Growth

Owing to the invasive procedures needed to obtain human lung tissue, animal models have been indispensible in the investigation of lung growth. From a mechanistic standpoint, major surgical lung resection (e.g., pneumonectomy), a

widely investigated model that consistently demonstrates robust compensatory growth of the remaining lung in all species examined including the mouse, rat, rabbit, ferret, dog [36–45], and indirectly in human subjects with functional loss of one lung [16, 17, 46–49]. Major lung resection mimics the loss of gas exchange units caused by obliterative disease, e.g., pulmonary fibrosis. However, unlike most models of lung injury, pneumonectomy removes a known and highly reproducible fraction of functioning lung units; the resulting signals and responses of the remaining lung units are readily quantifiable. Over more than a century, this model has been extensively characterized at physiological, structural, cellular, and molecular levels and utilized to study the sources and magnitudes of adaptation, the determinants of structural growth and remodeling as well as eventual functional outcome. Cumulative results strongly implicate mechanical stimuli in the re-initiation, modulation, and limitation of lung growth.

Pneumonectomy was first performed in dogs and rabbits in 1881, reviewed by [50]. By the 1920s, it was known that animals function quite well with one expanded remaining lung that fills the entire thoracic cavity [51–53], and surgeons began to perform major lung resection in patients. Studies in the 1950s showed that dogs [54] and patients [55] tolerate staged removal of up to 70 % of lung mass. Subsequently, rodents were used extensively for characterizing the cellular and molecular basis of accelerated post-pneumonectomy lung growth while the canine model remains useful for relating structure to function, defining the sources and limits of adaptation, and evaluating translational interventions.

Mechanical Signal–Response Relationships

In all species, the magnitude of post-pneumonectomy compensatory lung growth correlates inversely with age and maturation stage. Thus, compared to young animals compensatory growth in adults requires a higher threshold for initiation, a longer time course of adaptation [49] with early cell proliferation and progressive scaffold remodeling [56] that only partially normalizes structure–function [57, 58]. Critical pathways that are normally activated during lung development are further upregulated; nondevelopmental pathways may also be recruited [59]. The magnitude and distribution of compensatory growth vary with the fraction of lung units removed. Following canine left pneumonectomy (~42% resection), only the most caudal (infracardiac) remaining lobe exhibits significant growth of alveolar tissue and surface area; compensation is derived predominantly from alveolar-capillary recruitment and parenchyma remodeling. Following right pneumonectomy (58 % resection), alveolar growth intensifies in magnitude and uniformity in all lobes; compensatory gains in structure and function exceed that following 42 % resection [60]. Following 65–70 % lung resection, alveolar growth is still vigorous but with diminishing gains in structure and function [57] (Fig. 12.3). This pattern signifies a *threshold*, an *optimal range*, and an *upper limit* of the mechanical signal–response relationship following increasing loss of lung units.
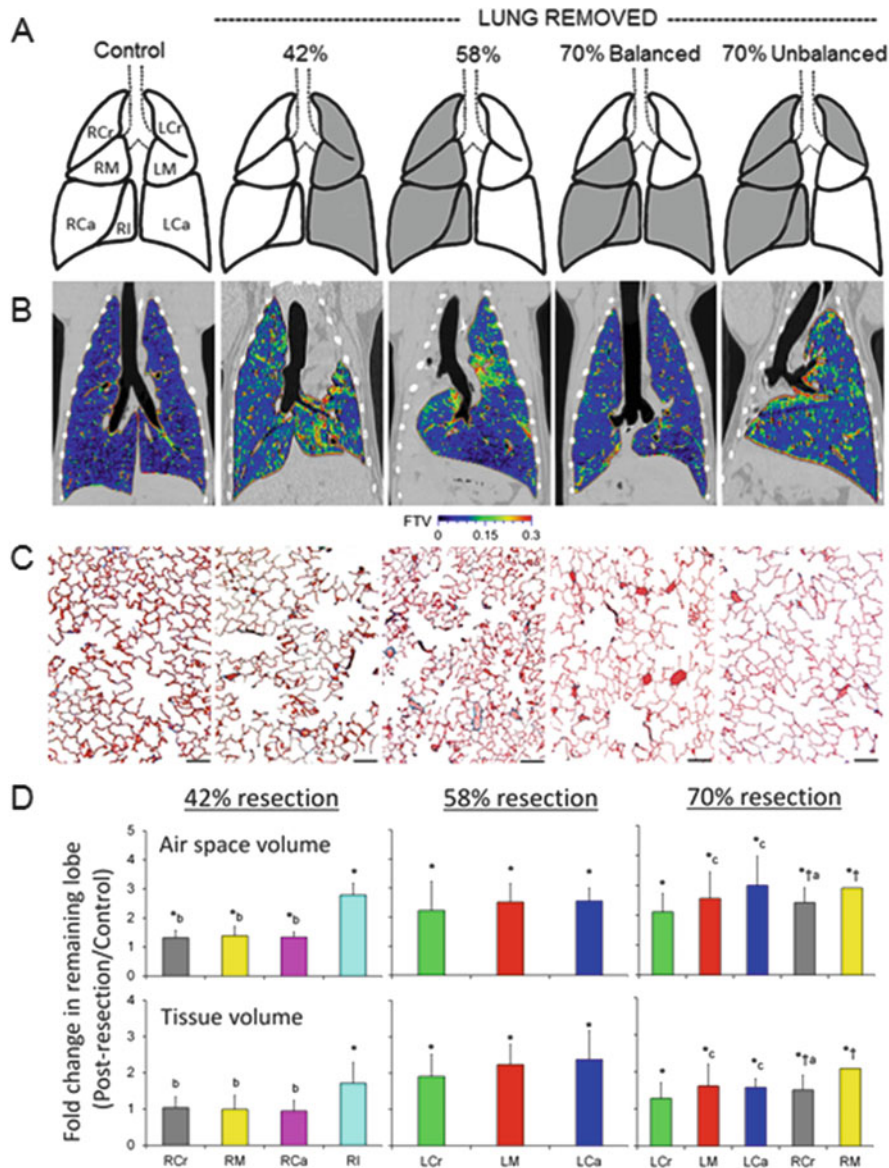
Fig. 12.3 Structural response to increasing loss of lung units by pneumonectomy—42, 58, and 70 % balanced and 70 % unbalanced resection. (**a**) The adult canine lobes removed are shaded in *gray*. (**b**) Coronal HRCT images are shown at the level of the carina. The *color scale* indicates in vivo fractional tissue volume (FTV) of lung parenchyma. (**c**) Representative micrographs of the distal lung. Bar = 200 μm. (**d**) Average fold changes in airspace volume (*upper*) and extravascular alveolar tissue volume (*lower*) in individual remaining lobes following different degrees of lung resection, expressed as ratios with respect to the same lobe in normal control animals. The lobes were fixed by tracheal instillation at a constant airway pressure. *Left*: 42 % resection. *Middle*: 58 % resection. *Right*: 70 % resection (balanced and unbalanced groups combined). *Right lobes*: *RCr* right cranial (*gray*), *RM* right middle (*yellow*), *RCa* right caudal (*magenta*), *RI* right infracardiac
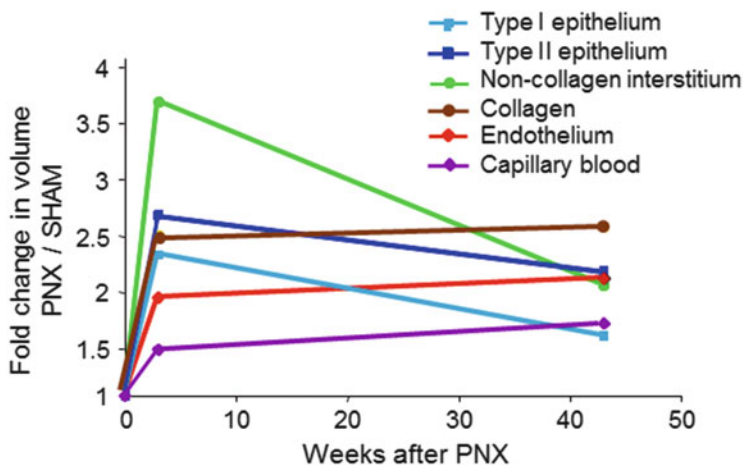
Fig. 12.4 Increases in the compartmental volumes of the alveolar septa in young dogs (2.5 months age) 3 weeks and 1 year following 58 % resection by right pneumonectomy (PNX), expressed as ratios to the corresponding mean values in litter- and gender-matched control animals following sham pneumonectomy. Note the early disproportionate increase in the volume of non-collagen septal interstitium

Following 42 % resection, lobar expansion initially unfolds the remaining alveolar septa with little tissue stress in most lobes except the infracardiac lobe, which lies between the heart and the diaphragm, preferentially expands across the midline, increases nearly twofold increase in tissue volume and partially reconstitutes the cardiac fossa. Type-2 pneumocyte volume increases first, before that of other septal cell types, suggesting its sensitivity to mechanical stress and consistent with its role as a resident progenitor cell [61]. Following 58 % lung resection, expansion and stress in all lobes exceed a critical threshold, leading to uniform growth initiation, stress relief, and greater functional enhancement per unit of initially remaining lung compared to 42 % resection. The initial rapid post-pneumonectomy airspace expansion is followed by further gradual expansion in the subsequent days as intrathoracic air and fluid are resorbed. An increase in tissue permeability recruits fluid, cells (especially monocytes and macrophages), chemokines, and cytokines to the remaining lung leading to a disproportionate (3.6-fold) increase in the volume of septal interstitial cells and matrix (excluding collagen). With time, the gain in interstitial volume wanes, and all major septal components—epithelium, interstitium, endothelium, and capillary blood—increase to about two (1.5–2.5) fold of that in the control lung (sham pneumonectomy) (Fig. 12.4). Signals related to airspace expansion account for approximately half of the observed post-pneumonectomy structure–function compensation (Fig. 12.5);

Fig. 12.3 (continued) (*aqua*). *Left lobes*: *LCr* left cranial (*green*), *LM* left middle (*red*), *LCa* left caudal (*blue*). Mean ± SD. $P \leq 0.05$: *vs. control (1.0); [†]vs. 42 %; [a]vs. RM, [b]vs. RI, [c]vs. LCr. Adapted from [57]
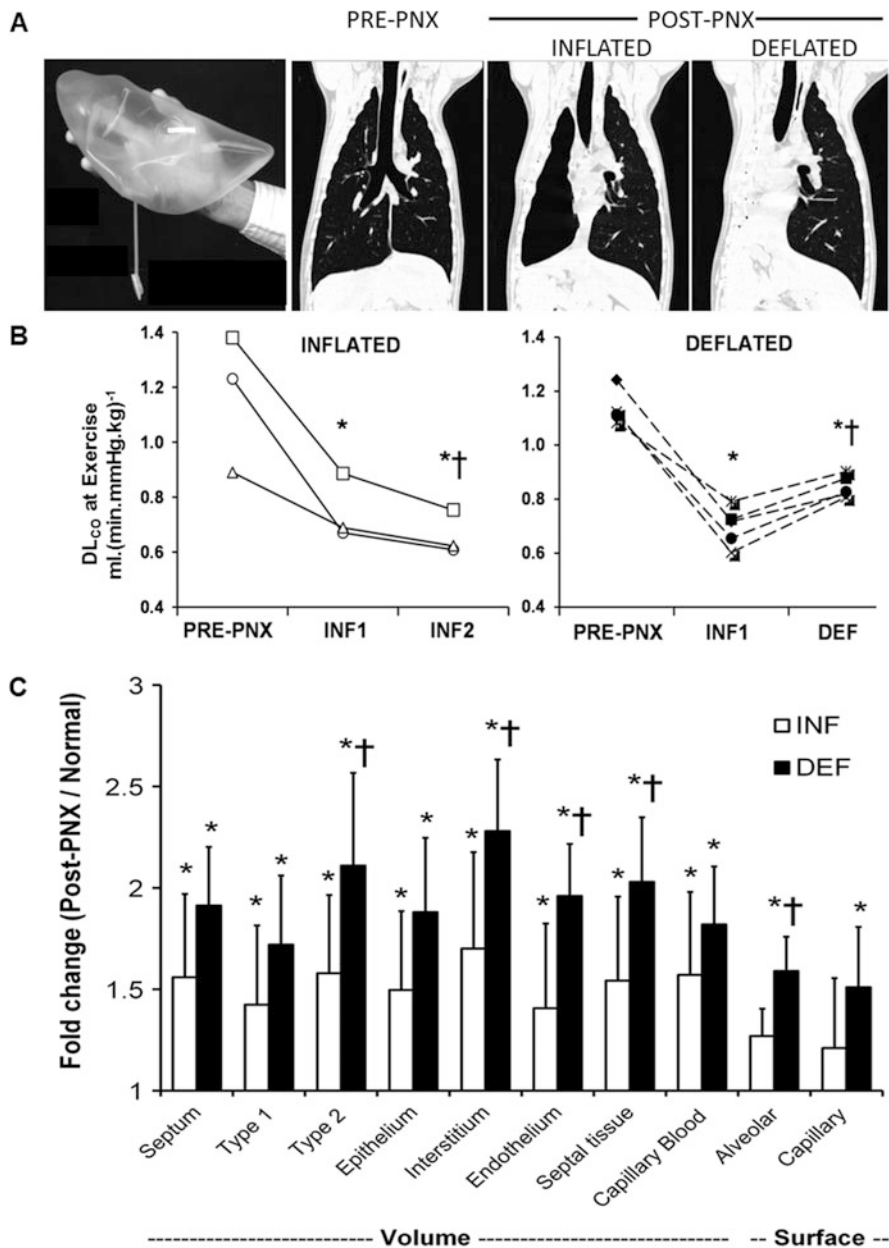
Fig. 12.5 Contribution of lung expansion to post-pneumonectomy (PNX) growth and compensation. *Upper panels*: Adult canine right lung was replaced with custom-shaped inflated silicone prosthesis following right PNX to minimize expansion of the remaining lobes. High-resolution computed tomography was performed at a transpulmonary pressure of 30 cmH$_2$O pre- and 4 months post-PNX (with inflated prosthesis, INF), and then 4 months following acute deflation of the prosthesis (~8 months after surgery, DEF). Control animals underwent right PNX with continuously inflated prosthesis and also studied at 4 and 8 months post-PNX (INF1 and INF2, respectively). *Middle*: Lung diffusing capacity (DL$_{CO}$) was measured during exercise and

the remainder is attributable to perfusion-related stimuli although nonmechanical factors may also play a role [62, 63]. As resection increases from 58 to 65–70 %, the diminishing gains in growth and compensation suggest the counter-balancing effects of excessive mechanical stress that may heighten cellular oxidative stress and damage tissue integrity at the expense of growth-related activities. An excessive increase in pulmonary vascular resistance may also impair tissue adaptive response. However, new capillaries (evidenced by an increase in double alveolar-capillary profiles) continue to form with increasing loss of lung units without reaching a plateau up to 70 % resection, suggesting the existence of separate perfusion-related stimuli for microvascular growth [57].

Quantifying Regional Mechanical Stimuli

Using in vivo high-resolution computed tomography, nonrigid image registration and deformation analysis, we visualized regional parenchyma deformation (displacement, strain, and shear) and compliance, and quantified growth of the functional parenchyma, which includes alveolar tissue as well as microvascular blood [56, 64]. Results demonstrate markedly nonuniform regional displacement, deformation, and growth with inflation (Fig. 12.6), with a prolonged course of adaptation marked by initial parenchyma growth, progressive tissue relaxation, stress relief, and gradual functional improvement over many months [56, 58, 64] (Fig. 12.7). A protracted temporal course of adaptation is probably fundamentally important to ensure the coordination and optimization of homeostatic pathways at micro and macro scales and to minimize architectural distortion. Intuitively, one might expect nonuniform spatial stimuli-response to weaken the average or the whole lung compensation at a given stimulus intensity. On the other hand, nonuniformity also prolongs the "*window of susceptibility*" during which mechanical stimuli remain active at least in some parts of the lung, thereby rendering the overall adaptive response amenable to intervention.

Structural Basis of Compensatory Growth and Remodeling

Postnatal compensatory lung growth is thought to be mediated mainly via recruitment and activation of resident progenitor cells in response to local signals while circulating bone marrow-derived cells or vascular progenitor cells play no role or at

Fig. 12.5 (continued) expressed at a constant cardiac output of 400 mL (min kg)$^{-1}$ in individual animals pre-PNX and at the two time-points post-PNX. $P \leq 0.05$: *vs. pre-PNX and †vs. INF1 by repeated measures ANOVA. *Lower*: Fold increase in volumes and surface areas of alveolar septal components measured 1 year following right PNX in animals with inflated or deflated prosthesis, expressed as ratios to the average values in normal controls. Mean ± SD. $P \leq 0.05$: *vs. control (1.0), †vs. INF. From [62, 63]
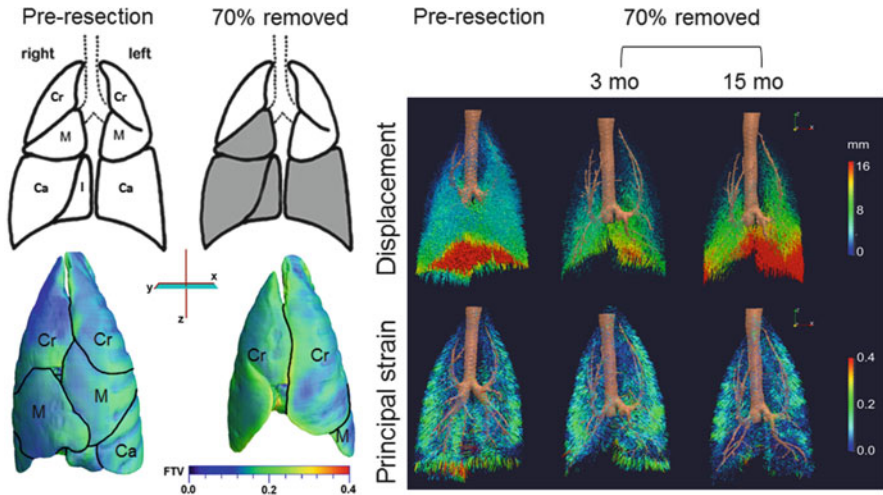
Fig. 12.6 Parenchyma deformation quantified by high-resolution computed tomography. *Left upper panels*: Diagrams of normal adult canine lobes and those remaining following balanced 70 % resection—the removed lobes are shaded in *gray*. *Left lower panels*: Representative three-dimensional reconstruction shows marked expansion of the remaining three lobes (demarcated by *black lines*) mainly in a caudal direction and around the mediastinum. The *color map* shows heterogeneous subpleural fractional tissue volume (FTV). Lobes: *Cr* cranial, *M* middle, *Ca* caudal. *Right panels*: Three-dimensional vector field maps of parenchyma displacement (*upper*) and principal strain (*lower*) during inflation (from 15 to 30 cmH$_2$O transpulmonary pressure) before and 3 and 15 months after 70 % resection illustrate temporal and spatial mechanical heterogeneity during compensation. At 3 months post-compared to pre-resection, displacement magnitude is reduced and principal strain increases nonuniformly in the enlarged remaining lobes compared to the same lobe pre-resection. At 15 months compared to 3 months post-resection, displacement increases markedly particularly in caudal regions, and regional strain is nonuniformly reduced [88, 89]

best a minor role [65–67]. Alveolar septation is a four-dimensional event involving spatio-temporal coordination of hundreds of genes and thousands of mediators. The bulk of gas exchange occurs through the "*thin side*" of septa, which contains minimal tissue with high barrier conductance. Structural support of septa is concentrated in the "*thick side*," which contains most of the cells, matrix, and fibers. As the elastin fibers coursing throughout the "*thick side*" of alveolar wall are pulled under tension, they may lift and "fold" an existing alveolar capillary, create a tissue pillar that transects the capillary lumen leading to a "double-capillary" profile typical of the developing lung. Tension on elastin fibers may also lift tissue and capillary constituents out of their two-dimensional plane to create a new septum. Subsequently, cell proliferation, matrix deposition, and fiber rearrangement separate the "double-capillary" and remodel it into two single capillaries typical of the mature lung. This process, termed "*intussusception*" [68], could generate a new septum or expand an existing alveolar tissue-capillary sheet depending on the balance of forces (Fig. 12.8).
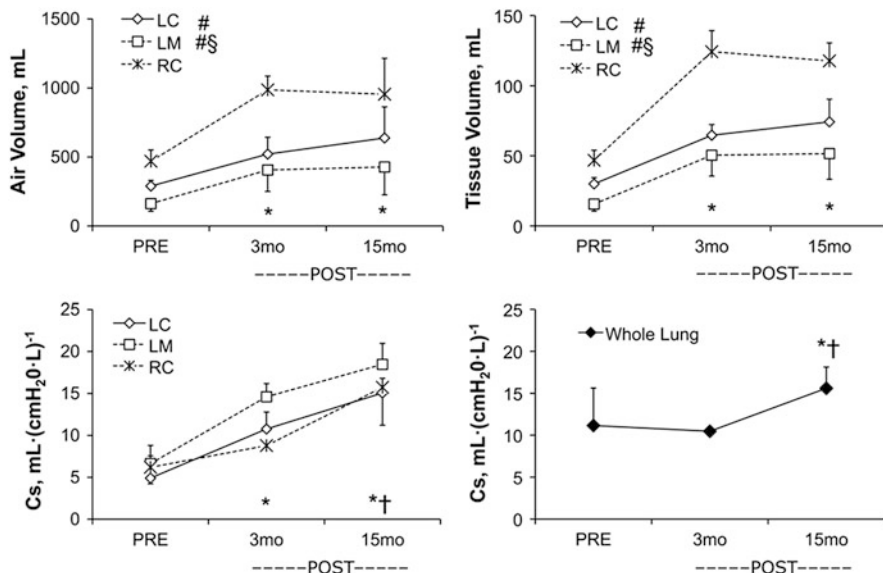
Fig. 12.7 Growth and remodeling phases in the remaining lobes 3 and 15 months following 65–70 % lung resection assessed by high-resolution computed tomography. *Upper panels*: Lobar air and tissue volumes increase significantly from PRE to 3 months POST-resection then remain stable between 3 and 15 months. *Lower left panel*: Specific compliance (Cs) of the remaining three lobes continue to increase from 3 to 15 months POST-resection. *Lower right panel*: Whole lung Cs (representing seven lobes PRE and three lobes POST) did not change from PRE to 3 months POST then increased between 3 and 15 months POST. Mean ± SD. *Lobes*: *RC* right cranial, *LC* left cranial, *LM* left middle. Repeated measures ANOVA with post hoc analysis by Fisher's Protected Least Significant Difference. Comparison with respect to time: $P < 0.05$, *vs. PRE, †vs. 3 months POST in all remaining lobes. Comparison among lobes: $P < 0.05$, #vs. RC, §vs. LC. From [56]

At the level of acinar airways, alveolar ducts contain smooth muscle and other contractile elements in their incomplete walls, which form the entrance rings to alveolar sacs [3]. Following pneumonectomy, alveolar ducts increase in number and volume [69]. Branching of the most distal alveolar ducts could add one more airway generation to double the total alveolar tissue volume and surface areas. This is a likely mechanism because tissue deformation is disproportionally larger in subpleural than central lung regions [56] corresponding to a similar gradient of cell proliferation and growth factor expression [12, 13]. Alternatively, alveolar sacs may bud from the terminal bronchiole that forms the entrance to an acinus, transforming the terminal bronchiole into another generation of respiratory bronchiole. It remains unclear which, or perhaps both, of these mechanisms are operative during compensatory growth.

At the level of the conducting broncho-vasculature, further branching is not possible. A different type of growth occurs post-pneumonectomy, namely traction-related elongation and dilatation, which must also involve the generation of additional tissue components. Elongation along each airway or vascular generation
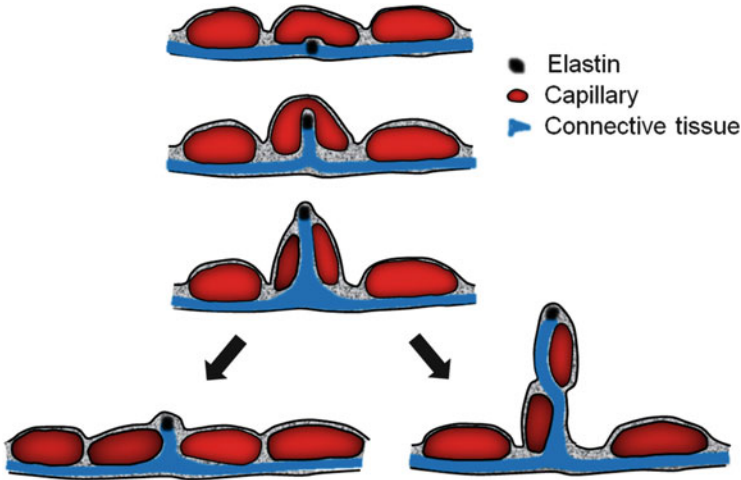
Fig. 12.8 Diagram of intussusceptive capillary growth and formation of a new alveolar septum. See text for explanation

increases, while dilatation mitigates, the increase in flow resistance. As luminal flow resistance is directly proportional to the length and inversely proportional to the fourth power of the radius (Poisuille's Law), only a small increase in radius is needed to offset the effects of lengthening. Bronchovascular adaptation is less vigorous or complete than alveolar adaptation, leading to dissociated compensation or "dysanaptic" lung growth [38, 70], where pulmonary limitation upon exercise is primarily limited by the persistently and disproportionately elevated airway and pulmonary vascular resistances and not by the reduction in lung diffusing capacity [71].

Species Differences in Lung Growth and Compensation

Large mammalian lungs differ from rodent lungs in several aspects of anatomy, development, and maturation that impact adaptation. Bronchovascular stratification is simplified in rodents. Respiratory bronchioles are few and short in the rabbit, guinea pig, hamster, gerbil, rat, and mice [72–74]. In human and canine lungs, acinar airways bifurcate through several generations of respiratory bronchioles and alveolar ducts to end in alveolar sacs. Extensive stratification allows modulation of ventilation–perfusion distributions and the penetration, deposition, and clearance of inhaled particles. Relative to rodent lungs, the highly stratified large lungs need stronger connective tissue and fibers for support, which in turn requires a more rigid rib cage to maintain stability but not too rigid as to restrict truncal flexibility in locomotion. Stratification also creates a longer mean acinar path length, which requires more smooth muscle and contractile elements to fine-tune ventilation–perfusion–diffusion matching among the regions and at different stratified levels. In

the vasculature, murine tracheobronchial capacitance vessels may not penetrate into intrapulmonary airways [75, 76], and perturbation of pulmonary blood flow readily stimulates angiogenesis of chest wall and pleural vessels [77]. In large animals, extensive bronchial and pulmonary precapillary anastomoses [78] provide ample collateral circulatory reserves, which may minimize the need for new vessel formation. These structural differences could explain the ease with which the lungs of small animals may be stimulated to regrow while the lungs of large animals rely heavily on nonstructural adaptive mechanisms; structural growth is stimulated only when the nonstructural reserves have been exhausted.

Translational Challenges in Lung Growth Induction

Mechanical signals are the only stimuli known to re-initiate adult lung growth de novo [5, 79]. While the innate growth potential is retained in adult lungs, the incomplete regrowth response is in need of ways of augmentation. This issue is critical because current therapy for chronic lung disease is non-curative except for lung transplantation, which is burdened by problems of donor availability and complications. The key unanswered questions include the following: (1) How to maximally realize the innate ability for regrowth and compensation of functioning lung units in obliterative disease and reduce the need for lung transplantation or replacement? (2) How to re-initiate lung growth in the absence of adequate mechanical stimuli such as in emphysema? (3) How to optimize alveolar cellular repopulation and capillary regrowth in bioengineered lungs?

The pneumonectomy model has proved useful for examining the integrated network interactions elicited by mechanical stimulation and for evaluating the efficacy of therapeutic approaches. Post-pneumonectomy exposure to ambient hypoxia [80, 81] and the administration of exogenous growth promoter molecules, proteins, and DNA [82, 83] have been shown to modestly enhance selective aspects of lung growth in rodents, although none has been shown to improve function. We examined this question in adult canines by administering oral all trans-retinoic acid (RA) for 3 months post-pneumonectomy. In the absence of active endogenous compensatory growth (left pneumonectomy), RA supplementation has no significant effect [83]. In the presence of endogenous growth activities (right pneumonectomy), RA supplementation modestly enhances growth of type-1 pneumocytes, interstitium, endothelium, and capillary blood volume as well as alveolar and capillary surface areas compared to placebo treatment [82, 84]. The expected increase in double-capillary profiles is also accentuated consistent with RA-enhanced capillary formation and remodeling. On the other hand, RA supplementation minimally stimulates the growth of alveolar type-2 pneumocytes, causes thickening of the alveolar-capillary basement membrane and the septa, and fails to significantly enhance long-term whole lung function [82, 84, 85]. These results suggest that pharmacological intervention could augment mechanically induced
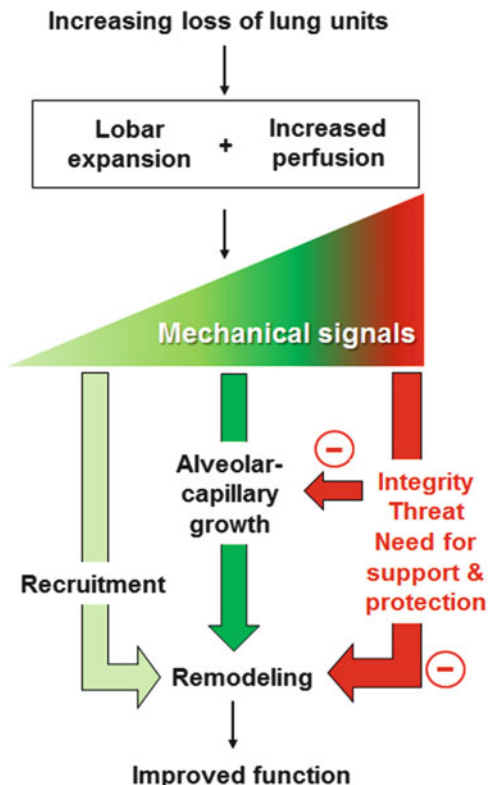
lung growth but is insufficient for re-initiating growth in the absence of sufficient mechanical signals. What factors prevent the translation of exogenously enhanced structural growth into functional gain? The answer remains speculative although a few possibilities should be considered:

1. Most studies tested a single exogenous growth promoter at a pharmacological dose over a short duration. This approach is conceptually inadequate because endogenous compensatory lung growth involves sustained, low-intensity, balanced amplification of numerous mechano-transduction pathways to gradually enlarge all parts of the gas exchanger, minimize distortion, and optimize outcome. Intense unbalanced stimulation could distort the blood gas barrier and neutralize the intended benefit. Broad stimulation of multiple key pathways at a low dose over a longer duration may be more effective in enhancing overall growth and function.
2. Scaffold remodeling continues long after cessation of accelerated cellular proliferation. As mechanical stress is redistributed and the local mechano-transduction micro-milieu shifts, different molecular pathways may be favored at different time points in the course of response. Selective administration of exogenous growth promoters that sequentially target each specific phase of the natural response may prove more effective.
3. Mechanical stimuli carry inherent risks of oxidative stress and tissue damage. Mildly increased mechanical lung stress (e.g., positive pressure breathing) is beneficial for maintaining airway patency. Moderate mechanical stress transduces growth and remodeling while excessive mechanical stress causes lung injury (e.g., ventilator-induced trauma). Balancing the competing adaptive needs—enlarging the gas exchange units vs. protecting the integrity of existing units—is a crucial part of the mechano-sensitive response spectrum (Fig. 12.9). For a given mechanical stress, the equilibrium interactions between signaling networks of growth/remodeling and those of cytoprotection determine the net gain in structure and function. Consistent with this idea, many of the endogenous growth/remodeling pathways that are upregulated post-pneumonectomy, e.g., hypoxia-inducible factor (HIF), erythropoietin (EPO), vascular endothelial growth factor (VEGF), and hepatocyte growth factor (HGF) [86–92], are multifunctional and simultaneously mediate cytoprotection. Strategies that aim to fortify cytoprotective pathways in addition to growth-promoting pathways may extend the upper limits of mechano-sensitive lung growth and function.

Implications for Chronic Lung Disease and Ex Vivo Lungs

Mechanically induced compensatory lung growth and remodeling enhances long-term gas exchange and mechanical function in adult mammals. Pharmacological manipulation [82, 83] and ambient hypoxia exposure [80, 81] modify already active growth-related pathways. When mechanical stimuli are *below* the growth-initiating threshold, these other attempts have little effect [83]. Thus, ambient hypoxia

Fig. 12.9 A paradigm for the spectrum of mechanically induced compensatory responses

Increasing loss of lung units

| Lobar expansion | + | Increased perfusion |

Mechanical signals

Alveolar-capillary growth

Recruitment

⊖ Integrity Threat Need for support & protection

Remodeling ⊖

Improved function

enhances lung growth and function in developing and not adult animals [93]. Young animals with an enlarging thorax respond more vigorously to pneumonectomy, and compensation is more complete, than older mature animals with fixed thoracic dimensions [94–96]. Exogenous growth factor supplementation enhances lung growth following 58 % and not 42 % resection [82–85]. Where mechanical signals are diminished as in pulmonary emphysema, attempts to pharmacologically stimulate lung growth have been uniformly unsuccessful. Whereas exogenous growth promoter modestly augments some aspects of mechanically induced lung growth, the response may be skewed leading to structural gain without functional enhancement. The fact that independent factors (maturity, hypoxia, parenchyma and vascular sources of mechanical stress) exert additive effects indicates plasticity of the innate regrowth potential and suggests possible approaches for augmentation. On the other hand, the risks of mechanically induced oxidative stress and tissue damage cannot be ignored. In interstitial lung disease, in addition to inflammation the typically patchy contracting fibrotic foci tether and deform the adjacent functioning alveoli, which can be expected to mechanically influence their adaptive response. Do these remaining functioning alveoli undergo compensatory growth/remodeling or suffer secondary physical injury compounding the primary insult? Perhaps both occur to varying degrees in different regions. Strategies that target the protection of

mechanically stressed remaining lung units might improve innate compensatory response as well as the response to exogenous interventions. In pulmonary emphysema, the priority will be to find novel ways of reconstituting normal mechano-transduction of the native lung. In ex vivo and bioengineered lungs, it will be imperative to optimize the magnitude and distribution of mechano-transduction response to facilitate cell repopulation and matrix remodeling as well as protect barrier integrity in all parts of the donor lung before and after in vivo implantation. Meeting these challenges require multi-scale integrated understanding of mechano-sensitive networks. There continues to be a need for models that mimic thoraco-pulmonary interactions in the human lung to bridge these knowledge gaps, test high impact interventions to harness the compensatory potential, and avoid translational failure when novel therapeutics are brought to human applications.

References

1. Ingber DE (2003) Tensegrity I. Cell structure and hierarchical systems biology. J Cell Sci 116:1157–1173
2. Weibel ER (2009) What makes a good lung? Swiss Med Wkly 139:375–386
3. Ochs M, Nyengaard JR, Jung A, Knudsen L, Voigt M, Wahlers T, Richter J, Gundersen HJ (2004) The number of alveoli in the human lung. Am J Respir Crit Care Med 169:120–124
4. Robertson HT, Altemeier WA, Glenny RW (2000) Physiological implications of the fractal distribution of ventilation and perfusion in the lung. Ann Biomed Eng 28:1028–1031
5. Hsia CC (2004) Signals and mechanisms of compensatory lung growth. J Appl Physiol 97:1992–1998
6. Unbekandt M, del Moral PM, Sala FG, Bellusci S, Warburton D, Fleury V (2008) Tracheal occlusion increases the rate of epithelial branching of embryonic mouse lung via the FGF10-FGFR2b-Sprouty2 pathway. Mech Dev 125:314–324
7. Papadakis K, Luks FI, De Paepe ME, Piasecki GJ, Wesselhoeft CW Jr (1997) Fetal lung growth after tracheal ligation is not solely a pressure phenomenon. J Pediatr Surg 32:347–351
8. Harding R, Hooper SB, Han VK (1993) Abolition of fetal breathing movements by spinal cord transection leads to reductions in fetal lung liquid volume, lung growth, and IGF-II gene expression. Pediatr Res 34:148–153
9. Tseng BS, Cavin ST, Booth FW, Olson EN, Marin MC, McDonnell TJ, Butler IJ (2000) Pulmonary hypoplasia in the myogenin null mouse embryo. Am J Respir Cell Mol Biol 22:304–315
10. Zhang S, Garbutt V, McBride JT (1996) Strain-induced growth of the immature lung. J Appl Physiol 81:1471–1476
11. Nobuhara KK, Fauza DO, DiFiore JW, Hines MH, Fackler JC, Slavin R, Hirschl R, Wilson JM (1998) Continuous intrapulmonary distension with perfluorocarbon accelerates neonatal (but not adult) lung growth. J Pediatr Surg 33:292–298
12. Massaro GD, Massaro D (1993) Postnatal lung growth: evidence that the gas-exchange region grows fastest at the periphery. Am J Physiol 265:L319–L322

13. Foster DJ, Yan X, Bellotto DJ, Moe OW, Hagler HK, Estrera AS, Hsia CCW (2002) Expression of epidermal growth factor and surfactant proteins during postnatal and compensatory lung growth. Am J Physiol Lung Cell Mol Physiol 283:L981–L990

14. Nagaya M, Akatsuka H, Kato J, Niimi N, Ishiguro Y (1996) Development in lung function of the affected side after repair of congenital diaphragmatic hernia. J Pediatr Surg 31:349–356

15. Beals DA, Schloo BL, Vacanti JP, Reid LM, Wilson JM (1992) Pulmonary growth and remodeling in infants with high-risk congenital diaphragmatic hernia. J Pediatr Surg 27:997–1001; discussion 1001–1002

16. Ijsselstijn H, Tibboel D, Hop WJ, Molenaar JC, de Jongste JC (1997) Long-term pulmonary sequelae in children with congenital diaphragmatic hernia. Am J Respir Crit Care Med 155:174–180

17. Marven SS, Smith CM, Claxton D, Chapman J, Davies HA, Primhak RA, Powell CV (1998) Pulmonary function, exercise performance, and growth in survivors of congenital diaphragmatic hernia. Arch Dis Child 78:137–142

18. McHugh K, Afaq A, Broderick N, Gabra HO, Roebuck DJ, Elliott MJ (2010) Tracheomegaly: a complication of fetal endoscopic tracheal occlusion in the treatment of congenital diaphragmatic hernia. Pediatr Radiol 40:674–680

19. Berend N, Marlin GE (1979) Arrest of alveolar multiplication in kyphoscoliosis. Pathology 11:485–491

20. Davies G, Reid L (1971) Effect of scoliosis on growth of alveoli and pulmonary arteries and on right ventricle. Arch Dis Child 46:623–632

21. Olgiati R, Levine D, Smith JP, Briscoe WA, King TK (1982) Diffusing capacity in idiopathic scoliosis and its interpretation regarding alveolar development. Am Rev Respir Dis 126:229–234

22. Boffa P, Stovin P, Shneerson J (1984) Lung developmental abnormalities in severe scoliosis. Thorax 39:681–682

23. Lund DP, Mitchell J, Kharasch V, Quigley S, Kuehn M, Wilson JM (1994) Congenital diaphragmatic hernia: the hidden morbidity. J Pediatr Surg 29:258–262; discussion 262–254

24. Xu J, Liu M, Liu J, Caniggia I, Post M (1996) Mechanical strain induces constitutive and regulated secretion of glycosaminoglycans and proteoglycans in fetal lung cells. J Cell Sci 109:1605–1613

25. Liu M, Xu J, Tanswell AK, Post M (1994) Inhibition of mechanical strain-induced fetal rat lung cell proliferation by gadolinium, a stretch-activated channel blocker. J Cell Physiol 161:501–507

26. Liu M, Qin Y, Liu J, Tanswell AK, Post M (1996) Mechanical strain induces pp60src activation and translocation to cytoskeleton in fetal rat lung cells. J Biol Chem 271:7066–7071

27. Chess PR, Toia L, Finkelstein JN (2000) Mechanical strain-induced proliferation and signaling in pulmonary epithelial H441 cells. Am J Physiol Lung Cell Mol Physiol 279:L43–L51

28. Sanchez-Esteban J, Tsai SW, Sang J, Qin J, Torday JS, Rubin LP (1998) Effects of mechanical forces on lung-specific gene expression. Am J Med Sci 316:200–204

29. Liu M, Liu J, Buch S, Tanswell AK, Post M (1995) Antisense oligonucleotides for PDGF-B and its receptor inhibit mechanical strain-induced fetal lung cell growth. Am J Physiol 269: L178–L184

30. Waters CM, Chang JY, Glucksberg MR, DePaola N, Grotberg JB (1997) Mechanical forces alter growth factor release by pleural mesothelial cells. Am J Physiol 272:L552–L557

31. Liu M, Skinner SJ, Xu J, Han RN, Tanswell AK, Post M (1992) Stimulation of fetal rat lung cell proliferation in vitro by mechanical stretch. Am J Physiol 263:L376–L383

32. Sanchez-Esteban J, Wang Y, Cicchiello LA, Rubin LP (2002) Cyclic mechanical stretch inhibits cell proliferation and induces apoptosis in fetal rat lung fibroblasts. Am J Physiol Lung Cell Mol Physiol 282:L448–L456

33. Breen EC (2000) Mechanical strain increases type I collagen expression in pulmonary fibroblasts in vitro. J Appl Physiol 88:203–209

34. Smith PG, Moreno R, Ikebe M (1997) Strain increases airway smooth muscle contractile and cytoskeletal proteins in vitro. Am J Physiol 272:L20–L27
35. Simon A, Tanaka EM (2013) Limb regeneration. Wiley interdisciplinary reviews. Dev Biol 2:291–300
36. Cagle PT, Thurlbeck WM (1988) Postpneumonectomy compensatory lung growth. Am Rev Respir Dis 138:1314–1326
37. Hsia CCW, Berberich MA, Driscoll B, Laubach VE, Lillehei CW, Massaro DJ et al (2004) Mechanisms and limits of induced postnatal lung growth. Am J Respir Crit Care Med 170:319–343
38. Hsia CC (2004) Lessons from a canine model of compensatory lung growth. Curr Top Dev Biol 64:17–32
39. Burri PH, Sehovic S (1979) The adaptive response of the rat lung after bilobectomy. Am Rev Respir Dis 119:769–777
40. Langston C, Sachdeva P, Cowan MJ, Haines J, Crystal RG, Thurlbeck WM (1977) Alveolar multiplication in the contralateral lung after unilateral pneumonectomy in the rabbit. Am Rev Respir Dis 115:7–13
41. Sekhon HS, Thurlbeck WM (1992) A comparative study of postpneumonectomy compensatory lung response in growing male and female rats. J Appl Physiol 73:446–451
42. Thurlbeck WM, Langston C (1989) Long-term consequences of compensatory lung growth. J Appl Physiol 66:2891–2894
43. Davies P, McBride J, Murray GF, Wilcox BR, Shallal JA, Reid L (1982) Structural changes in the canine lung and pulmonary arteries after pneumonectomy. J Appl Physiol 53:859–864
44. Kirchner KK, McBride JT (1990) Changes in airway length after unilateral pneumonectomy in weanling ferrets. J Appl Physiol 68:187–192
45. McBride JT (1985) Postpneumonectomy airway growth in the ferret. J Appl Physiol 58:1010–1014
46. Laros CD, Westermann CJ (1987) Dilatation, compensatory growth, or both after pneumonectomy during childhood and adolescence. A thirty-year follow-up study. J Thorac Cardiovasc Surg 93:570–576
47. Ciric I, Meyers MP, Mayba J, Anthonisen NR (2003) Autopneumonectomy with compensatory lung growth. Can Respir J 10:271–273
48. McBride JT, Wohl ME, Strieder DJ, Jackson AC, Morton JR, Zwerdling RG et al (1980) Lung growth and airway function after lobectomy in infancy for congenital lobar emphysema. J Clin Invest 66:962–970
49. Butler JP, Loring SH, Patz S, Tsuda A, Yablonskiy DA, Mentzer SJ (2012) Evidence for adult lung growth in humans. N Engl J Med 367:244–247
50. Schilling JA (1965) Pulmonary resection and sequelae of thoracic surgery. In: Fenn WO, Rahn H (eds) Handbook of physiology section 3: respiration. American Physiological Society, Washington, DC, pp 1531–1563
51. Heuer GJ, Dunn GR (1920) Experimental pneumonectomy. Bull Johns Hopkins Hosp 31:31–42
52. Heuer GJ, Andrus WDW (1922) Alveolar and blood gas changes following pneumonectomy. Bull Johns Hopkins Hosp 33:130–134
53. Andrus WDW (1923) Observations on the total lung volume and blood flow following pneumonectomy. Bull Johns Hopkins Hosp 34:119–121
54. Schilling JA, Harvey RB, Balke B, Rattunde HF (1956) Extensive pulmonary resection in dogs: altitude tolerance, work capacity, and pathologic-physiologic changes. Ann Surg 144:635–646
55. DeGraff AC Jr, Taylor HF, Ord JW, Chuang TH, Johnson RL Jr (1965) Exercise limitation following extensive pulmonary resection. J Clin Invest 44:1514–1522
56. Yilmaz C, Tustison NJ, Dane DM, Ravikumar P, Takahashi M, Gee JC, Hsia CC (2011) Progressive adaptation in regional parenchyma mechanics following extensive lung resection assessed by functional computed tomography. J Appl Physiol 111:1150–1158

57. Ravikumar P, Yilmaz C, Dane DM, Bellotto DJ, Estrera AS, Hsia CC (2014) Defining a stimuli-response relationship in compensatory lung growth following major resection. J Appl Physiol 116(7):816–824

58. Hsia CC, Herazo LF, Ramanathan M, Johnson RL Jr, Wagner PD (1993) Cardiopulmonary adaptations to pneumonectomy in dogs. II. VA/Q relationships and microvascular recruitment. J Appl Physiol 74:1299–1309

59. Zhang Q, Zhang J, Moe OW, Hsia CC (2008) Synergistic upregulation of erythropoietin receptor (EPO-R) expression by sense and antisense EPO-R transcripts in the canine lung. Proc Natl Acad Sci U S A 105:7612–7617

60. Hsia CCW, Herazo LF, Ramanathan M, Johnson RL Jr (1994) Cardiopulmonary adaptations to pneumonectomy in dogs. IV. Membrane diffusing capacity and capillary blood volume. J Appl Physiol 77:998–1005

61. Hsia CC, Johnson RL Jr (2006) Further examination of alveolar septal adaptation to left pneumonectomy in the adult lung. Respir Physiol Neurobiol 151:167–177

62. Dane DM, Yilmaz C, Estrera AS, Hsia CC (2013) Separating in vivo mechanical stimuli for postpneumonectomy compensation: physiological assessment. J Appl Physiol 114:99–106

63. Ravikumar P, Yilmaz C, Bellotto DJ, Dane DM, Estrera AS, Hsia CC (2013) Separating in vivo mechanical stimuli for postpneumonectomy compensation: imaging and ultrastructural assessment. J Appl Physiol 114:961–970

64. Yilmaz C, Ravikumar P, Dane DM, Bellotto DJ, Johnson RL Jr, Hsia CC (2009) Noninvasive quantification of heterogeneous lung growth following extensive lung resection by high-resolution computed tomography. J Appl Physiol 107:1569–1578

65. Voswinckel R, Ziegelhoeffer T, Heil M, Kostin S, Breier G, Mehling T et al (2003) Circulating vascular progenitor cells do not contribute to compensatory lung growth. Circ Res 93:372–379

66. Suga A, Ueda K, Takemoto Y, Nishimoto A, Hosoyama T, Li TS, Hamano K (2013) Significant role of bone marrow-derived cells in compensatory regenerative lung growth. J Surg Res 183:84–90

67. Eisenhauer P, Earle B, Loi R, Sueblinvong V, Goodwin M, Allen GB, Lundblad L, Mazan MR, Hoffman AM, Weiss DJ (2013) Endogenous distal airway progenitor cells, lung mechanics, and disproportionate lobar growth following long-term post-pneumonectomy in mice. Stem Cells 31:1330–1339

68. Burri PH (2006) Structural aspects of postnatal lung development—alveolar formation and growth. Biol Neonate 89:313–322

69. Hsia CCW, Zhou XS, Bellotto DJ, Hagler HK (2000) Regenerative growth of respiratory bronchioles in dogs. Am J Physiol Lung Cell Mol Physiol 279:L136–L142

70. Dane DM, Johnson RL Jr, Hsia CCW (2002) Dysanaptic growth of conducting airways after pneumonectomy assessed by CT scan. J Appl Physiol 93:1235–1242

71. Hsia CC, Dane DM, Estrera AS, Wagner HE, Wagner PD, Johnson RL Jr (2008) Shifting sources of functional limitation following extensive (70%) lung resection. J Appl Physiol 104:1069–1079

72. Juhos LT, Green DP, Furiosi NJ, Freeman G (1980) A quantitative study of stenosis in the respiratory bronchiole of the rat in NO2-induced emphysema. Am Rev Respir Dis 121:541–549

73. Bal HS, Ghoshal NG (1988) Morphology of the terminal bronchiolar region of common laboratory mammals. Lab Anim 22:76–82

74. Irvin CG, Bates JH (2003) Measuring the lung function in the mouse: the challenge of size. Respir Res 4:4

75. Widdicombe J (1996) The tracheobronchial vasculature: a possible role in asthma. Microcirculation 3:129–141

76. Mitzner W, Lee W, Georgakopoulos D, Wagner E (2000) Angiogenesis in the mouse lung. Am J Pathol 157:93–101

77. Weibel ER (1960) Early stages in the development of collateral circulation to the lung in the rat. Circ Res 8:353–376

78. Ochs M, Weibel ER (2008) Functional design of the human lung for gas exchange. In: Fishman AP, Elias JA, Fishman JA, Grippi MA, Senior RM, Pack AI (eds) Fishman's pulmonary diseases and disorders, 4th edn. McGraw Hill, New York, pp 23–69

79. Wirtz HR, Dobbs LG (2000) The effects of mechanical forces on lung functions. Respir Physiol 119:1–17

80. Hsia CCW, Polo Carbayo JJ, Yan X, Bellotto DJ (2005) Enhanced alveolar growth and remodeling in guinea pigs raised at high altitude. Respir Physiol Neurobiol 147:105–115

81. Burri PH, Weibel ER (1971) Morphometric estimation of pulmonary diffusion capacity. II. Effect of PO2 on the growing lung, adaption of the growing rat lung to hypoxia and hyperoxia. Respir Physiol 11:247–264

82. Ravikumar P, Dane DM, McDonough P, Yilmaz C, Estrera AS, Hsia CC (2011) Long-term post-pneumonectomy pulmonary adaptation following all-trans-retinoic acid supplementation. J Appl Physiol 110:764–773

83. Yan X, Bellotto DJ, Dane DM, Elmore RG, Johnson RL Jr, Estrera AS, Hsia CC (2005) Lack of response to all-trans retinoic acid supplementation in adult dogs following left pneumonectomy. J Appl Physiol 99:1681–1688

84. Yan X, Bellotto DJ, Foster DJ, Johnson RL Jr, Hagler HH, Estrera AS, Hsia CC (2004) Retinoic acid induces nonuniform alveolar septal growth after right pneumonectomy. J Appl Physiol 96:1080–1089

85. Dane DM, Yan X, Tamhane RM, Johnson RL Jr, Estrera AS, Hogg DC, Hogg RT, Hsia CCW (2004) Retinoic acid-induced alveolar cellular growth does not improve function after right pneumonectomy. J Appl Physiol 96:1090–1096

86. Toffoli S, Roegiers A, Feron O, Van Steenbrugge M, Ninane N, Raes M, Michiels C (2009) Intermittent hypoxia is an angiogenic inducer for endothelial cells: role of HIF-1. Angiogenesis 12:47–67

87. Zhang Q, Bellotto DJ, Ravikumar P, Moe OW, Hogg RT, Hogg DC et al (2007) Postpneumonectomy lung expansion elicits hypoxia-inducible factor-1alpha signaling. Am J Physiol Lung Cell Mol Physiol 293:L497–L504

88. Zhang Q, Moe OW, Garcia JA, Hsia CC (2006) Regulated expression of hypoxia-inducible factors during postnatal and postpneumonectomy lung growth. Am J Physiol Lung Cell Mol Physiol 290:L880–L889

89. Foster DJ, Moe OW, Hsia CC (2004) Upregulation of erythropoietin receptor during postnatal and postpneumonectomy lung growth. Am J Physiol Lung Cell Mol Physiol 287:L1107–L1115

90. Sakamaki Y, Matsumoto K, Mizuno S, Miyoshi S, Matsuda H, Nakamura T (2002) Hepatocyte growth factor stimulates proliferation of respiratory epithelial cells during postpneumonectomy compensatory lung growth in mice. Am J Respir Cell Mol Biol 26:525–533

91. Nakamura T, Sakai K, Nakamura T, Matsumoto K (2011) Hepatocyte growth factor twenty years on: much more than a growth factor. J Gastroenterol Hepatol 26:188–202

92. Sakurai MK, Lee S, Arsenault DA, Nose V, Wilson JM, Heymach JV, Puder M (2007) Vascular endothelial growth factor accelerates compensatory lung growth after unilateral pneumonectomy. Am J Physiol Lung Cell Mol Physiol 292:L742–L747

93. Johnson RL Jr, Cassidy SS, Grover RF, Schutte JE, Epstein RH (1985) Functional capacities of lungs and thorax in beagles after prolonged residence at 3,100 m. J Appl Physiol 59:1773–1782

94. Takeda S, Hsia CCW, Wagner E, Ramanathan M, Estrera AS, Weibel ER (1999) Compensatory alveolar growth normalizes gas exchange function in immature dogs after pneumonectomy. J Appl Physiol 86:1301–1310

95. Takeda S, Ramanathan M, Wu EY, Estrera AS, Hsia CCW (1996) Temporal course of gas exchange and mechanical compensation after right pneumonectomy in immature dogs [published corrigenda in J. Appl. Physiol. 80(6): after table of contents, 1996.]. J Appl Physiol 80:1304–1312

96. Takeda S, Wu EY, Epstein RH, Estrera AS, Hsia CCW (1997) In vivo assessment of changes in air and tissue volumes after pneumonectomy. J Appl Physiol 82:1340–1348